MAGNETOTELLURIC MODEL STUDY OF PRISMATIC RESISTIVITY INHOMOGENEITIES IN A LAYERED EARTH

GL03303

Performed for

Diamond Shamrock Thermal Power Company
3333 Mendocino Avenue, Suite 120
Santa Rosa, California 95401

by

Philip E. Wannamaker
Howard P. Ross

August, 1985

CONTENTS

	Page
INTRODUCTION	1
NUMERICAL MODELS	2
CALCULATED RESULTS	3
Model A - Thick conductive prism at a depth of 1 km.	
Model B - Thick resistive prism at a depth of 1 km.	
Model C - Thin conductive prism at a depth of 1 km.	
Model D - Thick conductive prism at a depth of 1.5 km.	
CONCLUSIONS	8
REFERENCES	9

ILLUSTRATIONS

Figure 1. Thick (1 km wide) prism model, 1 km deep.

Figure 2. Thin (250 m wide) conductive prism, 1 km deep.

Figure 3. Thick conductive (1 ohm-m) 3-D body buried at a depth of 1 km.

Figure 4. Thick conductive (1 ohm-m) 2-D body buried at a depth of 1 km.

Figure 5. Thick resistive (20 ohm-m) 3-D body buried at a depth of 1 km.

Figure 6. Thick resistive (20 ohm-m) 2-D body buried at a depth of 1 km.

Figure 7. Thin conductive (0.5 ohm-m) 3-D body buried at a depth of 1 km.

Figure 8. Thin conductive (0.5 ohm-m) 2-D body buried at a depth of 1 km.

Figure 9. Thick conductive (1 ohm-m) 2-D body buried at a depth of 1.5 km.

INTRODUCTION

This report describes the results of a magnetotelluric model study which considered some simple prismatic inhomogeneities in an otherwise layered earth. Both conductive and resistive structures of limited strike extent (3-D) and infinite strike extent (2-D) were simulated. The purpose of this study is to demonstrate the amplitude, lateral spatial extent and frequency range of anomalies produced by the chosen models and, in particular, to recommend station spacing in a CSAMT/MT survey adequate to resolve such structures.

The three-dimensional prisms of this study were simulated using the integral equations algorithm of Wannamaker et al. (1984a), suitable for one or a few 3-D bodies in an arbitrarily layered host. Some additional MT model studies using this program which may be of interest to the reader have been published by Wannamaker et al. (1984b). The 2-D calculations were done with the finite element program of Wannamaker et al. (1985). This program can model arbitrary 2-D cross-sections including topography.

The present study was completed under Thermal Power Company Purchase Order No. 7306. The numerical models were computed on the Earth Science Laboratory/University of Utah Research Institute (ESL/UURI) Prime 400 computer. Drs. Wannamaker and Ross completed this study as private individuals rather than as ESL/UURI employees. Initial plans called for the computation of both wide and narrow conductive bodies at a depth of 1.5 km in addition to the bodies 1.0 km deep. Higher than anticipated

computer costs required a modification whereby one thick 2-D prism was modeled at a depth of 1.5 km. The probable responses of other bodies at a depth of 1.5 km can be inferred from the present results and basic formulations, and are discussed in this report.

NUMERICAL MODELS

Principal views of the three-dimensional prisms of this study are provided in Figures 1 and 2. Dashed lines indicate the discretization of the inhomogeneities into cells for simulation using the 3-D integral equations program. Both a conductive (1 ohm-m) and a relatively resistive (20 ohm-m) thick (1 km wide) prism were modeled. Also considered was a thin (250 m wide), somewhat more conductive (0.5 ohm-m) body. The depth to the top of these bodies is 1 km and their strike extent is 2 km. The two-dimensional structures were of identical cross-section to the 3-D prisms. All inhomogeneities were contained in the same layered earth, which is a 5 ohm-m half-space overlain by a 200 m thick resistive veneer of 500 ohm-m. Finally, to give some information on the effect of depth of burial, a 2-D thick conductive prism at a depth of 1.5 km was modeled.

The conductive bodies are intended to represent zones of enhanced fracturing and fluid content in the host rock, with the thinner body denoting a narrower zone. The resistive prism models a zone of reduced permeability and fluid content due, for instance, to igneous diking. In accordance with CSAMT surveys in general, a frequency range of 0.1 to 1 000 Hz was chosen over

which to perform the calculations. To sample the frequency dependence of the anomalies, results were run every one-half decade in frequency (i.e., f = 0.1, 0.3, 1., 3., ..., 1 000.) for most models. However, it turns out that the inhomogeneities do not produce visible anomalies for frequencies greater than about 10 Hz, so that calculations every full decade in frequency were completed in the upper half of the frequency range for the 3-D bodies to reduce unnecessary expense.

CALCULATED RESULTS

Quantities considered here are the apparent resistivities ρ_{xy} and ρ_{yx} and the impedence phases ϕ_{xy} and ϕ_{yx}, where x is the strike direction and y is to the right (Wannamaker et al, 1984b). For 2-D bodies and the symmetric 3-D geometries studied here, ρ_{xy} and ϕ_{xy} refer to the transverse electric (TE) mode in which the incident electric field is parallel to strike. Similarly, ρ_{yx} and ϕ_{yx} refer to the transverse magnetic (TM) mode in which the incident electric field is perpendicular to strike.

Also calculated were two functions of the vertical magnetic field over the inhomogeneities, denoted by the symbols T_H and T_E. The former is the magnitude of the vertical magnetic field normalized by the magnetic field in the y-direction (normal to strike) while the latter is the magnitude of the vertical field normalized by the electric field in the x-direction (along strike). Both T_H and T_E are transverse electric quantities. Finally, all results are presented as psuedosections, wherein station location along the y-axis serves as the abscissa and log frequency serves

as the ordinate for contour plots of amplitude or phase.

Model A.

Model A is the thick conductive body buried at a depth of 1 km (Figure 1). The MT response in psuedosection form for the 3-D body and its 2-D analog appear in Figures 3 and 4.

A fundamental characteristic of all psuedosections of ρ_{xy} and ρ_{yx} in this study is a progression from values around 300 ohm-m at the highest frequencies to less than 6 ohm-m by 0.1 Hz. This monotonic variation is due to the layered host containing the inhomogeneities, whereby the resistivity of the upper layer (500 ohm-m) dominates the high frequency results while that of the lower layer (5 ohm-m) dominates the low frequencies. In a corresponding fashion, ϕ_{xy} and ϕ_{yx} progress from values near 75° at the highest frequencies to values near 50° at the lowest. Values of impedance phase greater than 45° indicate apparent resistivities are decreasing as frequency decreases.

The buried inhomogeneities will be detectable according to the departures they cause from the layered earth response. For the 3-D body, a depression in ρ_{xy} of about 20% at the lowest frequency accompanies a positive anomaly in phase ϕ_{xy} of about 4° just below 1 Hz. The anomalous character of ρ_{yx} and ϕ_{yx} is similar to the TE quantities but is somewhat stronger (25% and 5°) and is more confined to an area immediately over the inhomogeneity. The vertical magnetic field function T_H exhibits quite small values, peaking around 0.02 at 0.3 Hz. The values of T_E exceed 5 Siemens (S) at the lowest frequency, but we do not know

what the typical statistical accuracy of this quantity is in field surveys. T_H and T_E are zero for purely layered earths.

The corresponding 2-D anomalies in Figure 4 are qualitatively similar to the 3-D ones, but slightly larger in amplitude. Also, impedance phase ϕ_{xy} at 0.1 Hz is very close to that of the layered host, while ϕ_{xy} for the 3-D case is still greater than the layered value, and the 2-D response in fact will fall below the layered earth phase at even lower frequencies. In a complementary fashion, ρ_{xy} for the 2-D body will return to the apparent resistivity of the layered host at frequencies below 0.1 Hz, while this 3-D quantity will remain depressed to arbitrarily low frequencies. This is perhaps the most striking difference between 2-D and 3-D MT responses for the TE mode (Wannamaker et al., 1984b). The TM mode results are relatively insensitive to strike length which makes them more reliable for 2-D interpretation (op. cit.). The effect of strike length is even more apparent in T_H and T_E, where the lesser volume of currents and the depression of anomalous current density by short strike length leads to 3-D results which are vey much less than the corresponding 2-D values (Wannamaker et al., 1984b).

Model B.

Model B is the thick resistive prism buried at a depth of 1 km (Figure 1). The MT responses for the 3-D body and its 2-D analog appear in Figures 5 and 6.

Since this body is resistive, the anomalous character of the MT response is of the opposite sense to that of a conductive inhomogeneity. Apparent resistivity highs over and near the body

increase at lower frequencies, with ρ_{yx} being somewhat more anomalous than ρ_{xy} (20% vs 10%). In a related fashion, impedance phase lows occur over the body and are most anomalous around 1 Hz. The anomaly in ϕ_{xy} for the 3-D body is less than 2° and that of ϕ_{yx} about 3°. Also, both T_H and T_E are much less for the resistive body than for the conductive since lesser anomalous current flow exists for the former.

The 2-D response in ρ_{xy} is no greater than for the 3-D case, and at 0.1 Hz we see that the 2-D anomaly is decaying and values are returning to those of the layered earth. In fact, a small positive anomaly in ϕ_{xy} has emerged at 0.1 Hz. This difference in ρ_{xy} and ϕ_{xy} between the 2-D and 3-D structures is analogous to, but of the opposite sense from, that described for the conductive bodies of Figures 3 and 4. For the 2-D body, ρ_{yx} and ϕ_{yx} are significantly more anomalous than for the 3-D. Values of ϕ_{yx} less than 45° occur over the body below 0.3 Hz and ρ_{yx} here is actually increasing. The vertical magnetic field functions T_H and T_E are greater for the 2-D body as expected, but the anomalies still are much smaller than for the conductive models.

Model C.

Model C is the thin conductive body of Figure 2 and the psuedosections of its response appear in Figures 7 and 8.

The responses of this narrower body are qualitatively similar to those of the thick conductor in Figures 3 and 4 but the anomalies of the former are smaller. This is especially so for ρ_{yx} and ϕ_{yx} (the TM mode) for both 2-D and 3-D geometries. The prism is much narrower than it is deep and an inducing

electric field across this smaller dimension does not produce a large current dipole moment. The vertical magnetic field functions T_H and T_E are less for the thin conductor than for the thick one, but they still are stronger than for the thick resistive body. In contrast to both models A and B, the TE response of model C is greater than the TM response.

Model D.

Model D is a conductive (1 ohm-m) 2-D prism, 1 km wide, simulated to provide some information on the effect of depth of burial on the MT response. The results of this model appear in Figure 9.

As anticipated, the anomalies of the deeper structure are broader in lateral extent, weaker in amplitude, and occur at lower frequencies than for a similar body at a depth of 1 km (Figure 4). The increase in breadth is between 50 and 100%, which is approximately the increase in depth. The reduction in amplitude is about the same. However, the frequencies at which the deeper body responds most strongly are lower than for model A by a factor of two to three. For the model prisms considered in this study, both 2-D and 3-D, the skin depth or depth of penetration of the incident field determines the frequency f below which the response occurs. This skin depth is proportional to $\sqrt{f}$, so that deepening the body by a certain factor tends to reduce the frequency of response by that factor squared. The response of this deeper body is truly at the low end of the CSAMT range. Furthermore, the finite strike length of the 3-D bodies we studied would result in an even steeper reduction in anomaly

amplitude as a body is deepened, perhaps by a factor of two or more, although the broadening of the anomaly at the surface would be about the same as for the 2-D case.

CONCLUSIONS

The responses of the resistivity inhomogeneities of this study are subtle and lie partially below the frequency range of available CSAMT surveying, i.e. 0.5 or 0.25 Hz. CSAMT is still preferred to MT as an exploration technique for the Puna area due to the lesser expense and greater ease of mobilization. If the targets in nature are only modestly wider or shallower than the models considered here, the chances of CSAMT being successful in their delineation will improve substantially. Nevertheless, excellent quality data to the lowest frequency possible (0.5 or 0.25 Hz) is essential. Resolution of apparent resistivity anomalies no greater than 20% or of phase anomalies no greater than 4° may be necessary.

For all models except the narrow conductive model C, the transverse magnetic mode (electric field perpendicular to strike) produces stronger anomalies which are more localized over the target than does the transverse electric mode. However, structures much narrower than their depth can only be resolved in the TE mode. A station spacing of no larger than one-half kilometer in a profile line is needed for anomaly resolution, and one-third kilometer is preferred. The station line spacing may be greater than this according to the length-to-width ratio of the targets sought.

REFERENCES

Wannamaker, P. E., Hohmann, G. W., and San Filipo, W. A., 1984a, Electromagnetic modeling of three-dimensional bodies in layered earths using integral equations: Geophysics, **49**, 60-74.

Wannamaker, P. E., Hohmann, G. W., and Ward, S. H., 1984b, Magnetotelluric responses of three-dimensional bodies in layered earths: Geophysics, **49**, 1517-1533.

Wannamaker, P. E., Stodt, J. A., and Rijo, L., 1985, PW2D-finite element program for solution of magnetotelluric responses of two-dimensional earth resistivity structure: Univ. of Utah Research Institute/Earth Science Laboratory Rep. ESL-158.

Figure 1. Thick (1 km wide) prism model, 1 km deep.

Figure 2. Thin (250 m wide) conductive prism model, 1 km deep.

Figure 3. Thick conductive (1 ohm-m) 3-D body buried at a depth of 1 km. a) TE mode. b) TM mode. c) TH, TE.

Figure 4. Thick conductive (1 ohm-m) 2-D body buried at a depth of 1 km. a) TE mode. b) TM mode. c). TH, TE.

Figure 5. Thick resistive (20 ohm-m) 3-D body buried at a depth of 1 km. a) TE mode. b) TM mode. c). TH, TE.

Figure 6. Thick resistive (20 ohm-m) 2-D body buried at a depth of 1 km. a) TE mode. b) TM mode. c). TH, TE.

Figure 7. Thin conductive (0.5 ohm-m) 3-D body buried at a depth of 1 km. a) TE mode. b) TM mode. c). TH, TE.

Figure 8. Thin conductive (0.5 ohm-m) 2-D body buried at a depth of 1 km. a) TE mode. b) TM mode. c). TH, TE.

Figure 9. Thick conductive (1 ohm-m) 2-D body buried at a depth of 1.5 km. a) TE mode. b) TM mode. c). TH, TE.

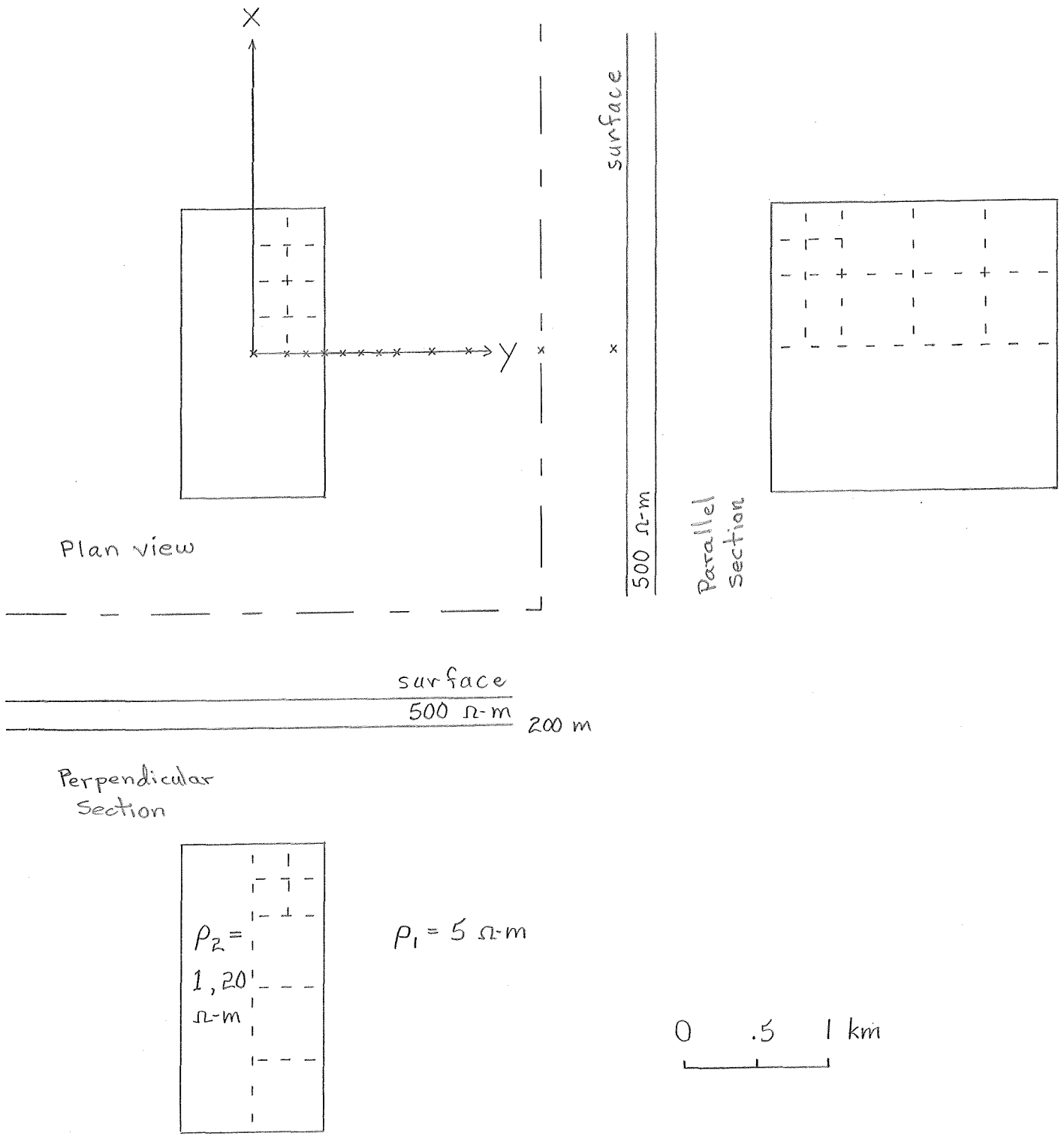

Figure 1. Thick (1 km wide) prism model, 1 km deep.

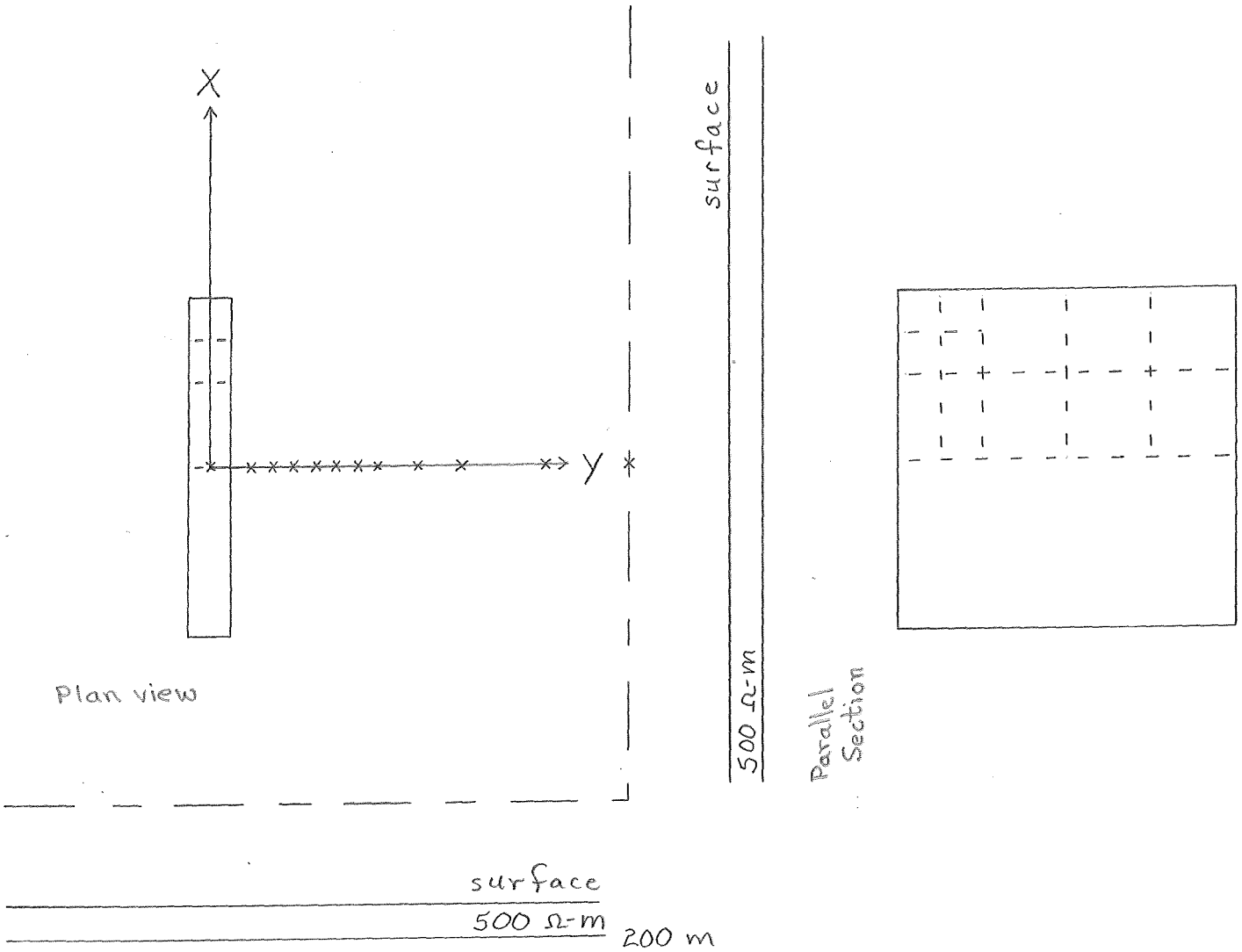

Figure 2. Thin (250 m wide) conductive prism model, 1 km deep.

	1	2	3	4	5	6	7	8	9	10	11	12	13	14	15	16	17	18	19	20	21	22	23	24	25	26	27	28	29	30	31	32	33	34	35	36	37	38	39	40
							3		7			1 km																													
	100 000	100 000	30 000	30 000	10 000	3000	1000	500	500	500	250	250	125	125	125	125	125	125	125	125	125	125	125	125	125	125	125	125	250	250	500	500	500	1000	3000	10 000	30 000	50 000	100 000	150 000
1	10																																							
2	30																																							
3	60																																							
4	70																																							
5	50																																							
6	30	50																																						
7	70	100																																						
8	150	250																																						
9	300	450																																						
10	200	300																																						
11	100	150																																						
12	160																																							
13	200																																							
14	400																																							
15	600																																							
16	400																																							
17	200																																							
18	100																																							
19	120																																							
20	480																																							
21	1200																																							
22	4000																																							
23	12 000																																							
24	40 000																																							
25	120 000																																							

500 (1)

5(2)

1.(3)

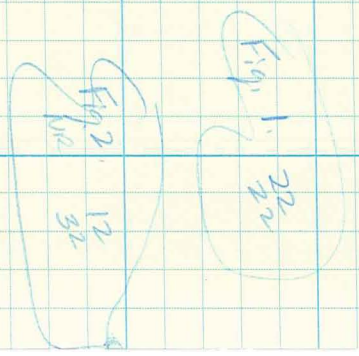

C

	1	2	3	4	5	6	7	8	9	10	11	12	13	14	15	16	17	18	19	20	21	22	23	24	25	26	27	28	29	30	31	32	33	34	35	36	37	38	39	40	41	42	43	44
								3km									500		250		100																								
	100 000	100 000	30 000	30 000	10 000	3000	1000	500	500	500	250	250	125	125	125	125	125	125	62.5	62.5	62.5	62.5	62.5	62.5	62.5	62.5	125	125	125	125	125	125	250	250	500	500	500	1000	3000	10 000	30 000	30 000	100 000	100 000

1	10
2	30
3	60
4	70
5	30
6	30
7	70
8	150
9	300
10	200
11	100
12	100
13	200
14	400
15	600
16	400
17	200
18	100
19	120
20	400
21	1200
22	4000
23	12 000
24	40 000
25	120 000

500 (1)

5 (2)

0.5 (3)

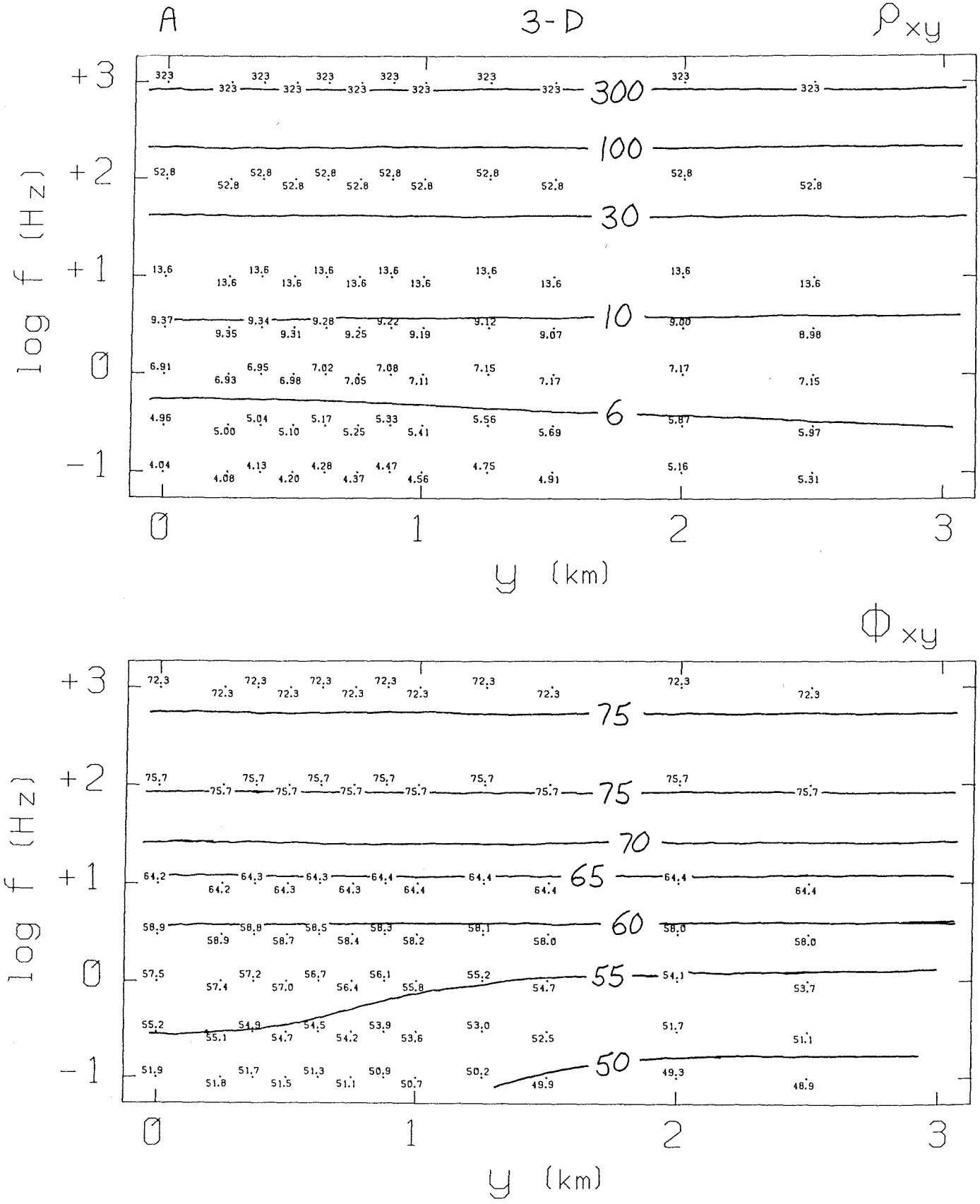

Figure 3. Thick conductive (1 ohm-m) 3-D body buried at a depth of 1 km. a) TE mode. b) TM mode. c) TH, TE.

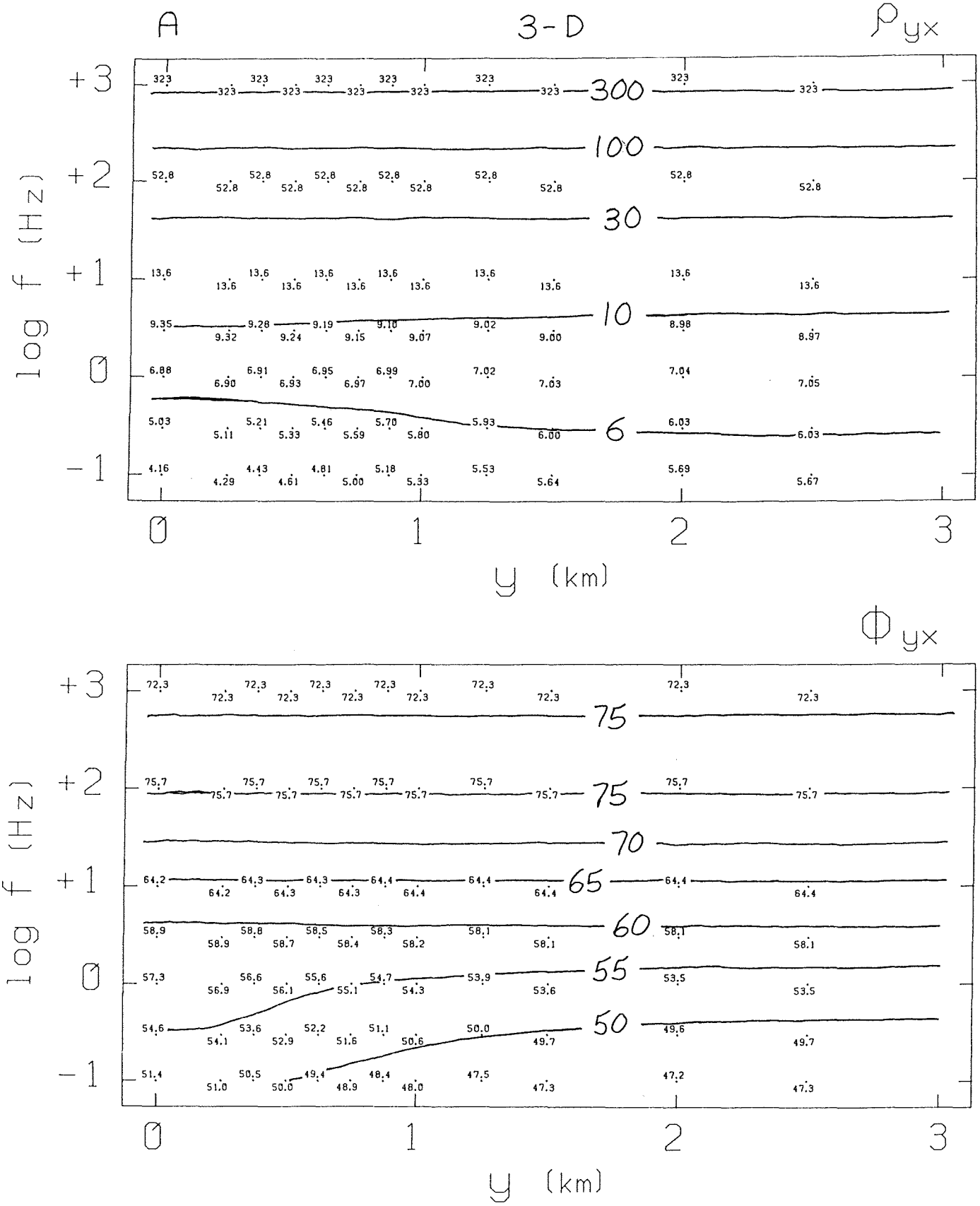

Figure 3. Thick conductive (1 ohm-m) 3-D body buried at a depth of 1 km. a) TE mode. b) TM mode. c) TH, TE.

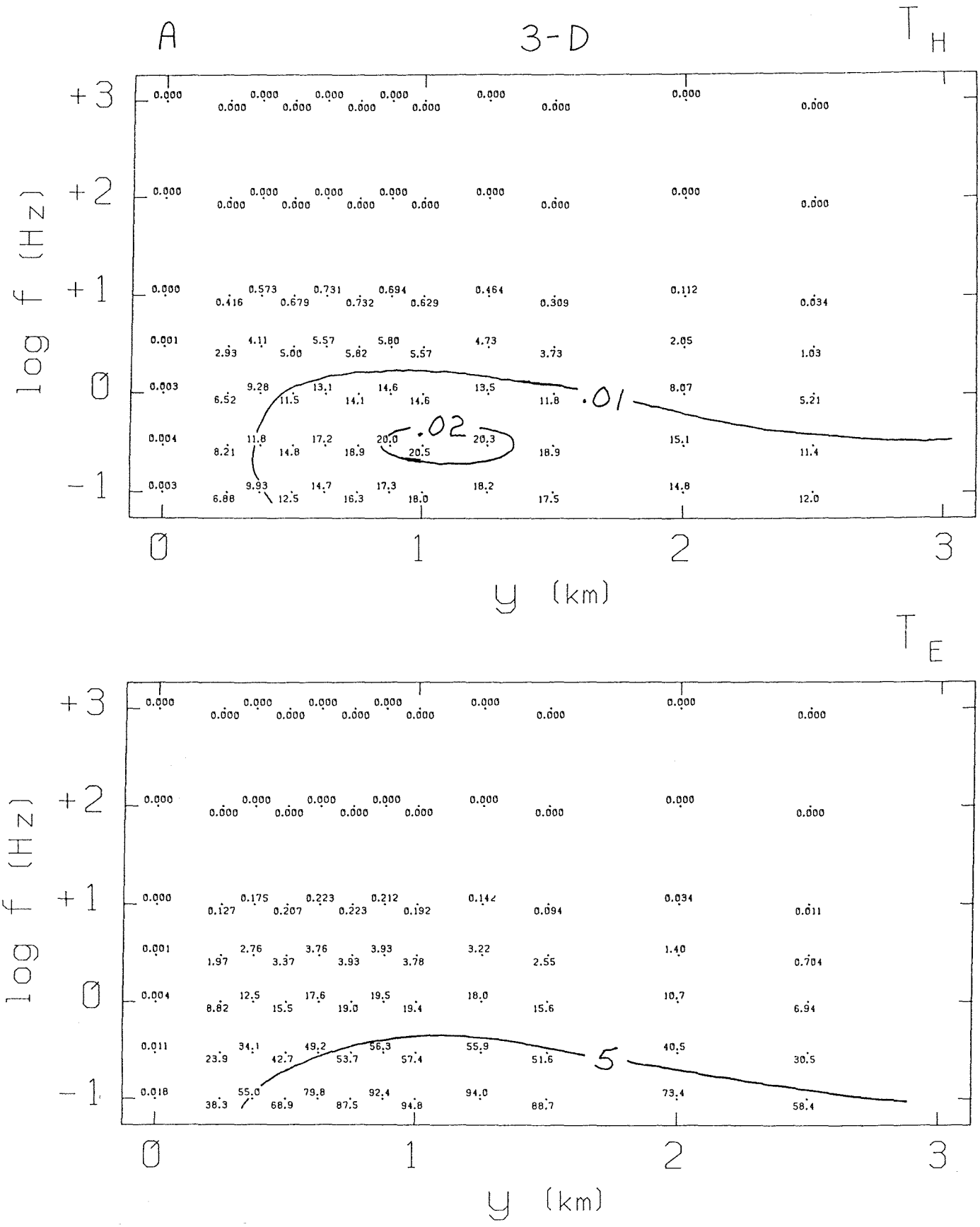

Figure 3. Thick conductive (1 ohm-m) 3-D body buried at a depth of 1 km. a) TE mode. b) TM mode. c) TH, TE.

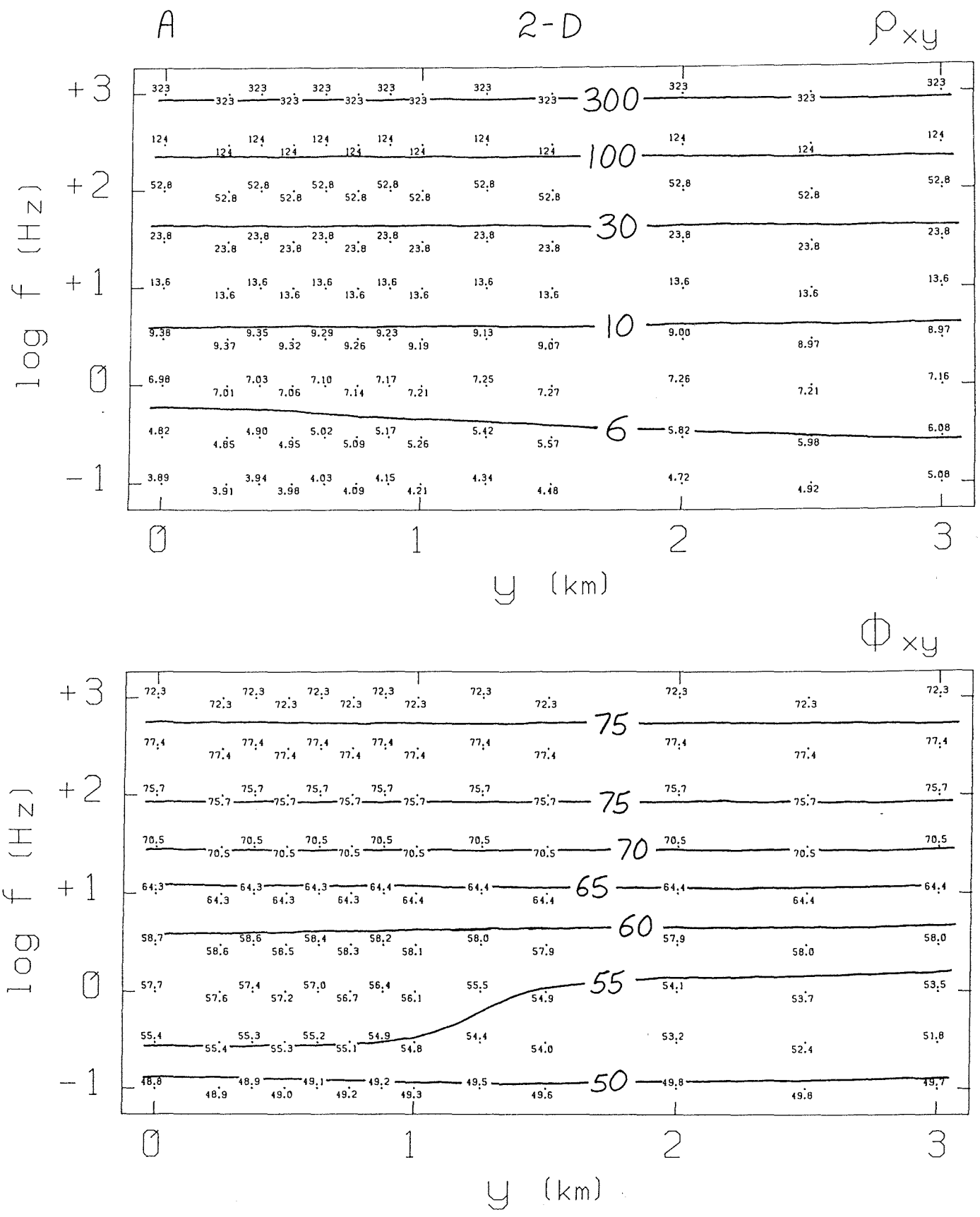

Figure 4. Thick conductive (1 ohm-m) 2-D body buried at a depth of 1 km. a) TE mode. b) TM mode. c). TH, TE.

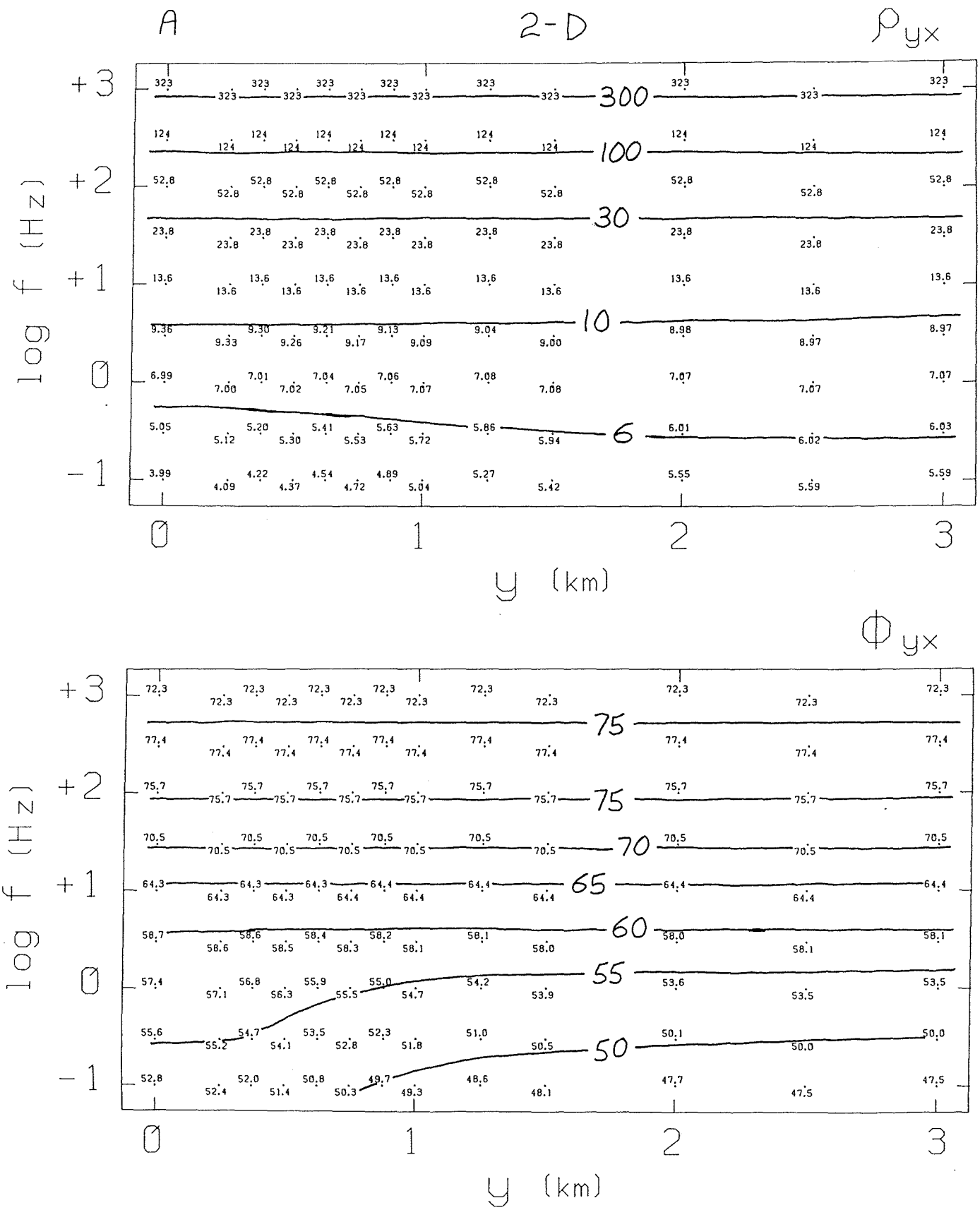

Figure 4. Thick conductive (1 ohm-m) 2-D body buried at a depth of 1 km. a) TE mode. b) TM mode. c). TH, TE.

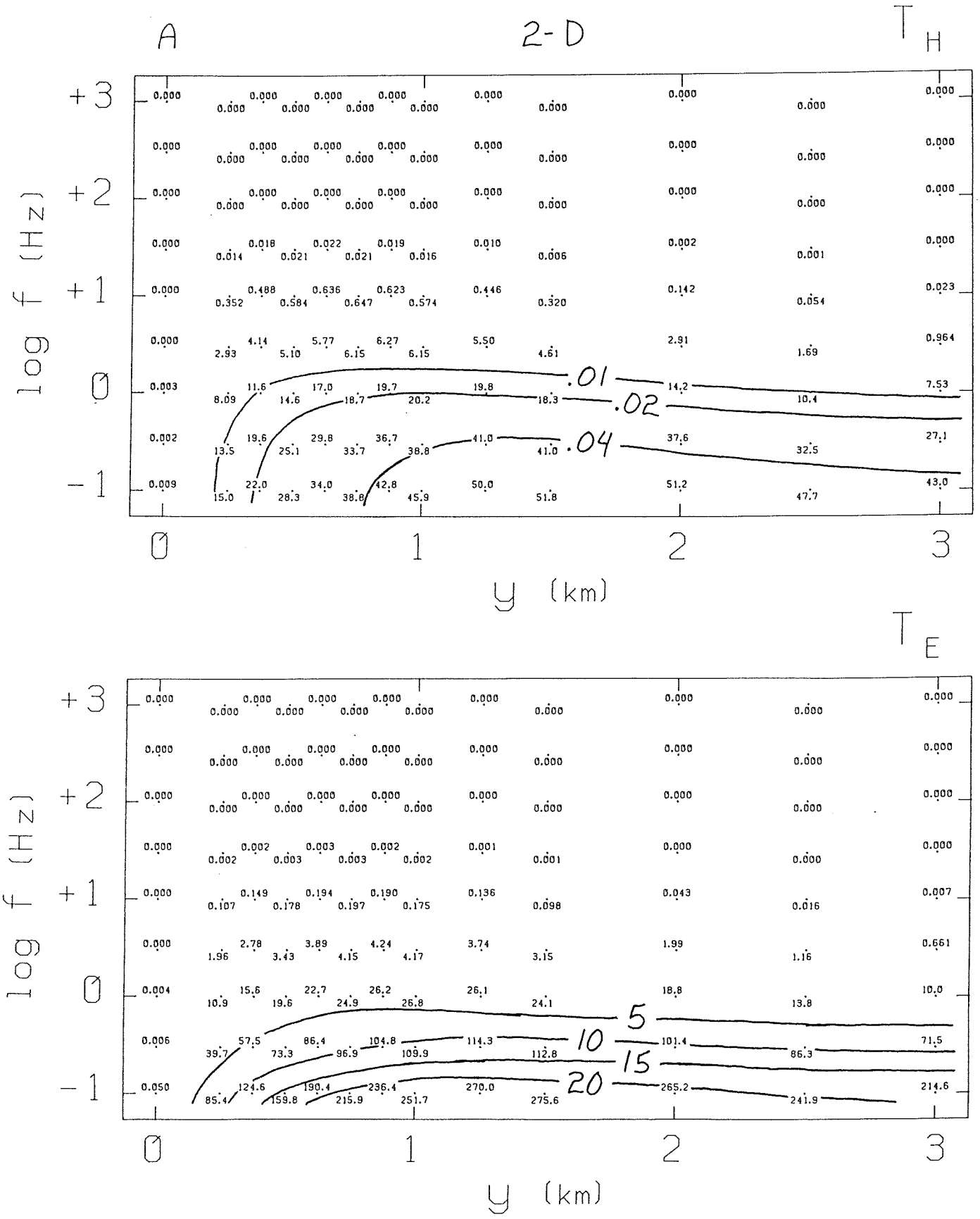

Figure 4. Thick conductive (1 ohm-m) 2-D body buried at a depth of 1 km. a) TE mode. b) TM mode. c). TH, TE.

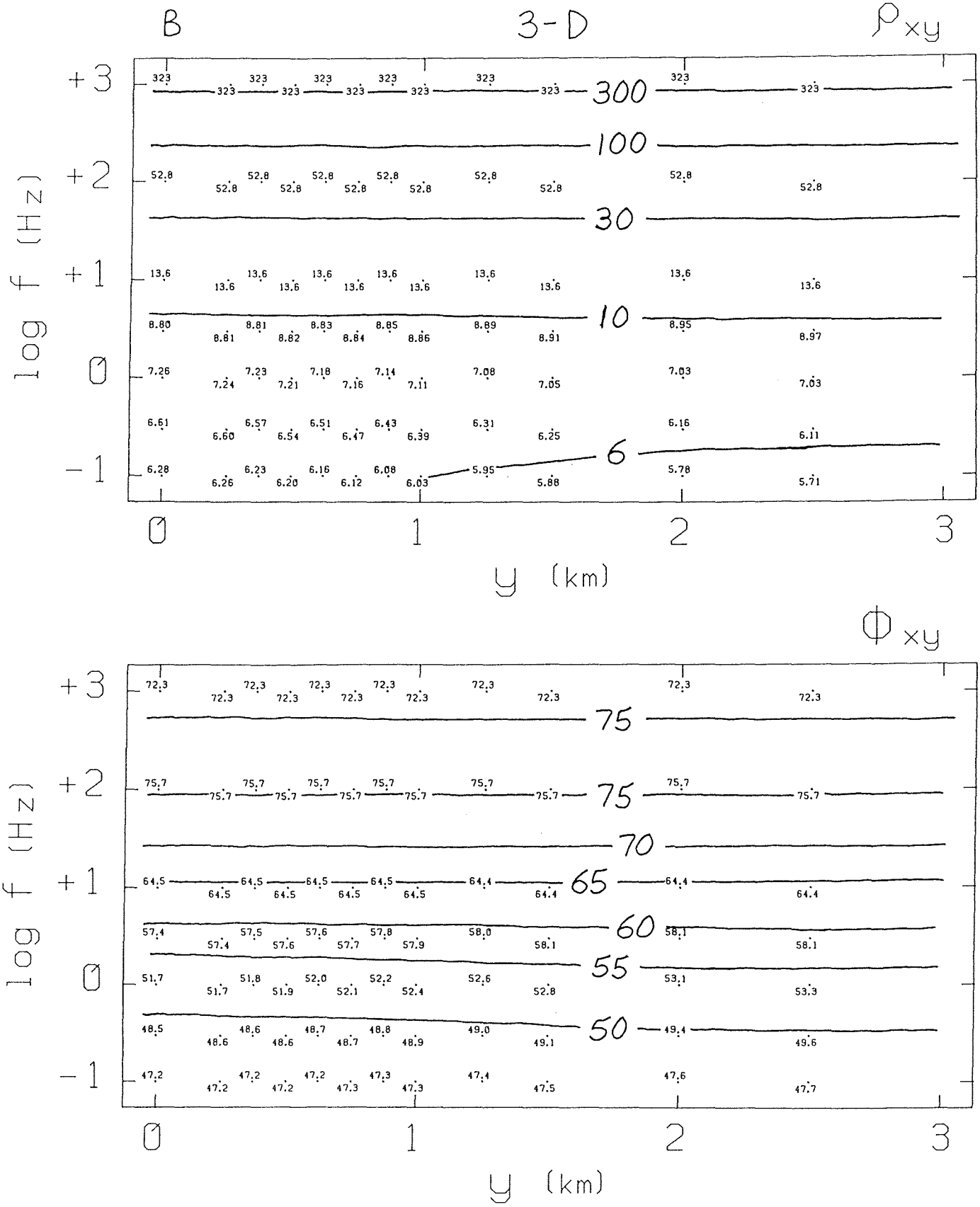

Figure 5. Thick resistive (20 ohm-m) 3-D body buried at a depth of 1 km. a) TE mode. b) TM mode. c). TH, TE.

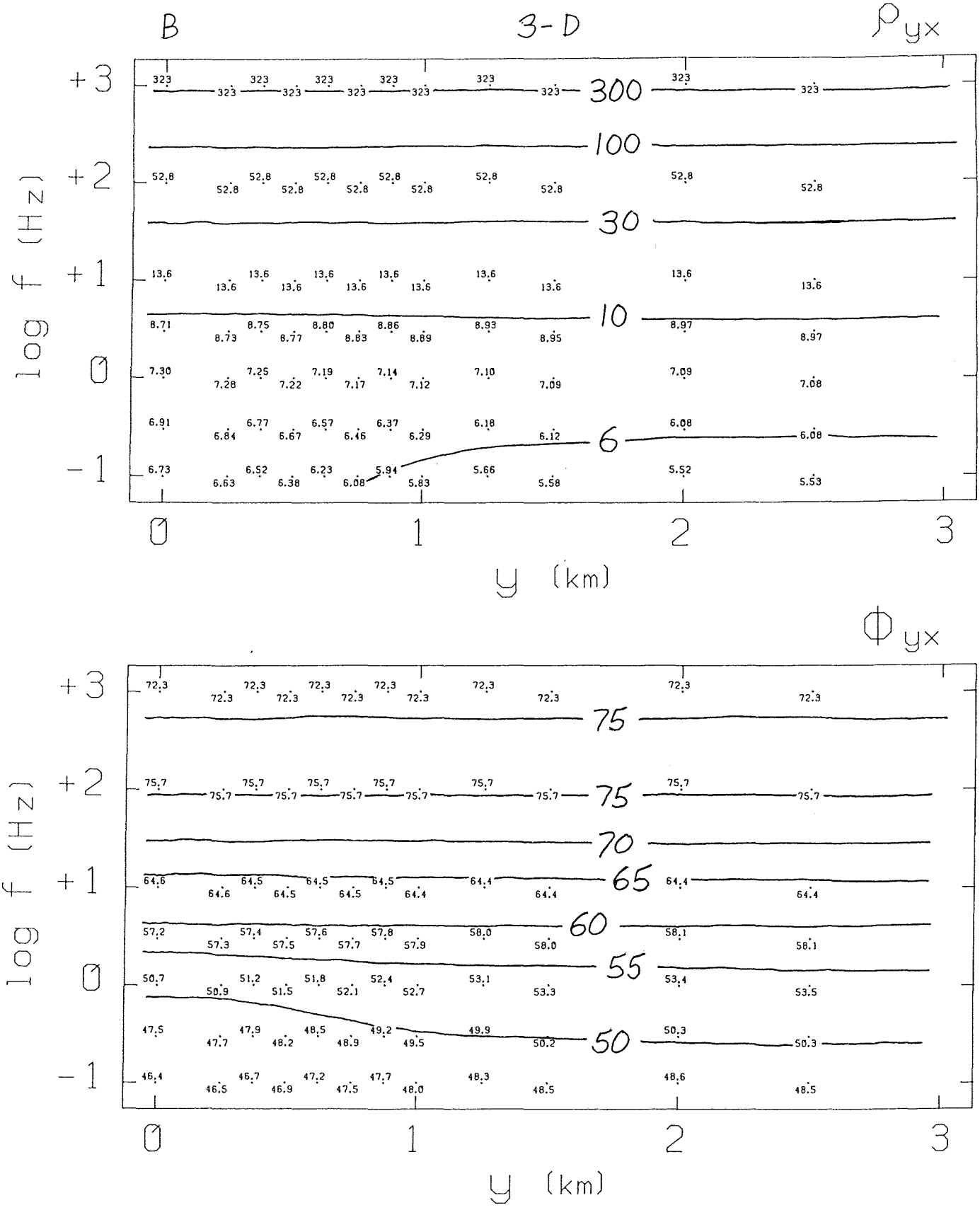

Figure 5. Thick resistive (20 ohm-m) 3-D body buried at a depth of 1 km. a) TE mode. b) TM mode. c). TH. TE.

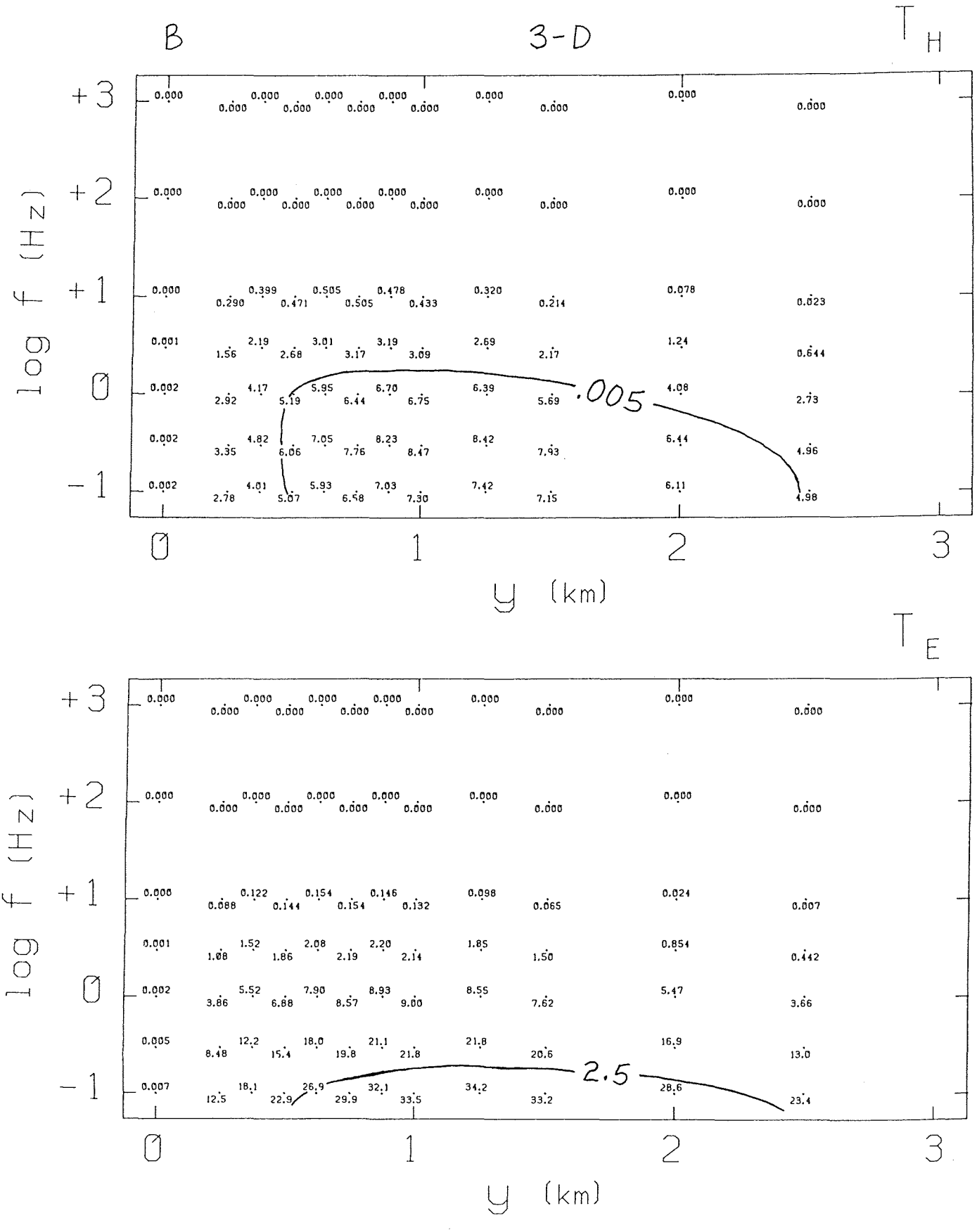

Figure 5. Thick resistive (20 ohm-m) 3-D body buried at a depth of 1 km. a) TE mode. b) TM mode. c). TH, TE.

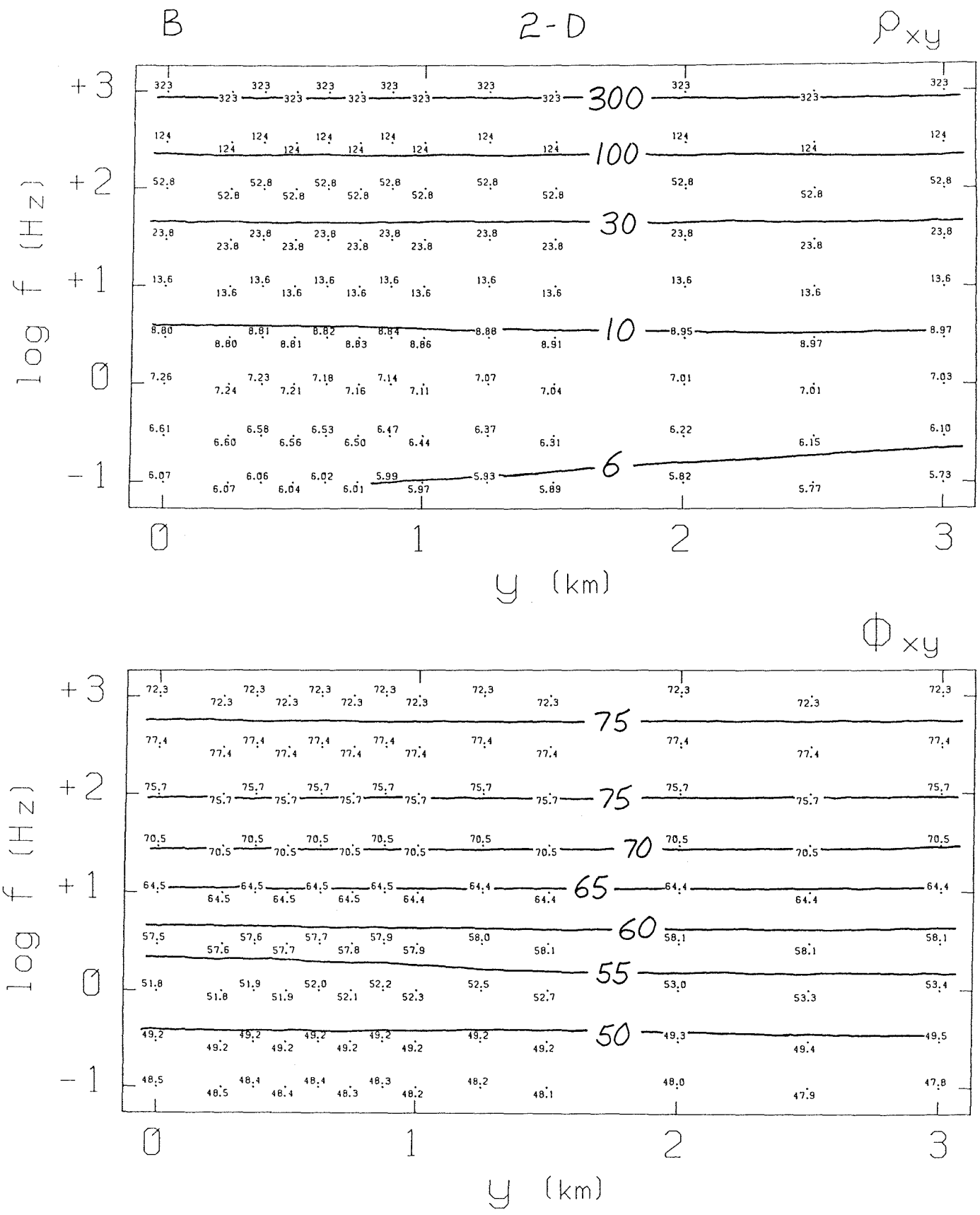

Figure 6. Thick resistive (20 ohm-m) 2-D body buried at a depth of 1 km. a) TE mode. b) TM mode. c). TH, TE.

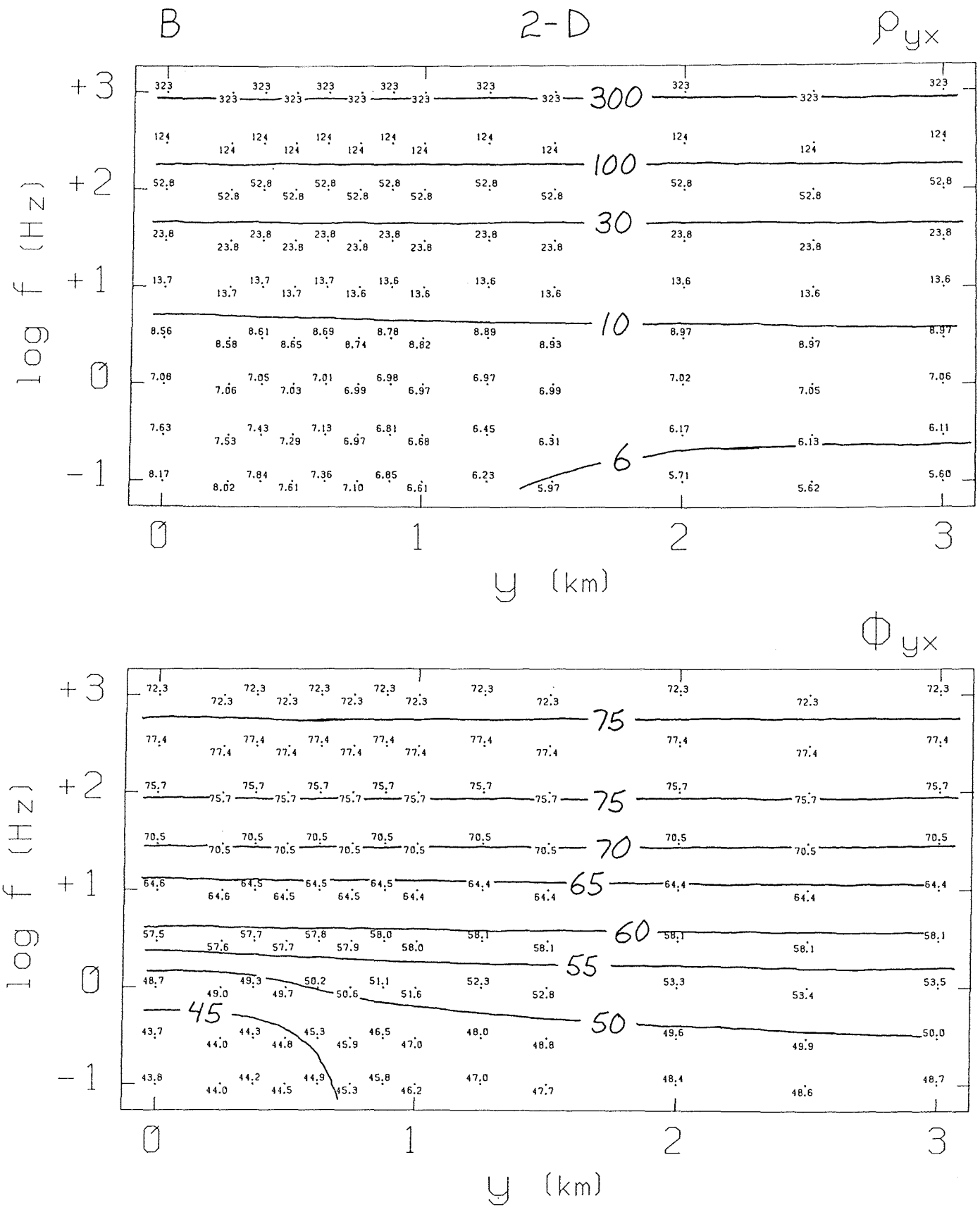

Figure 6. Thick resistive (20 ohm-m) 2-D body buried at a depth of 1 km. a) TE mode. b) TM mode. c). TH, TE.

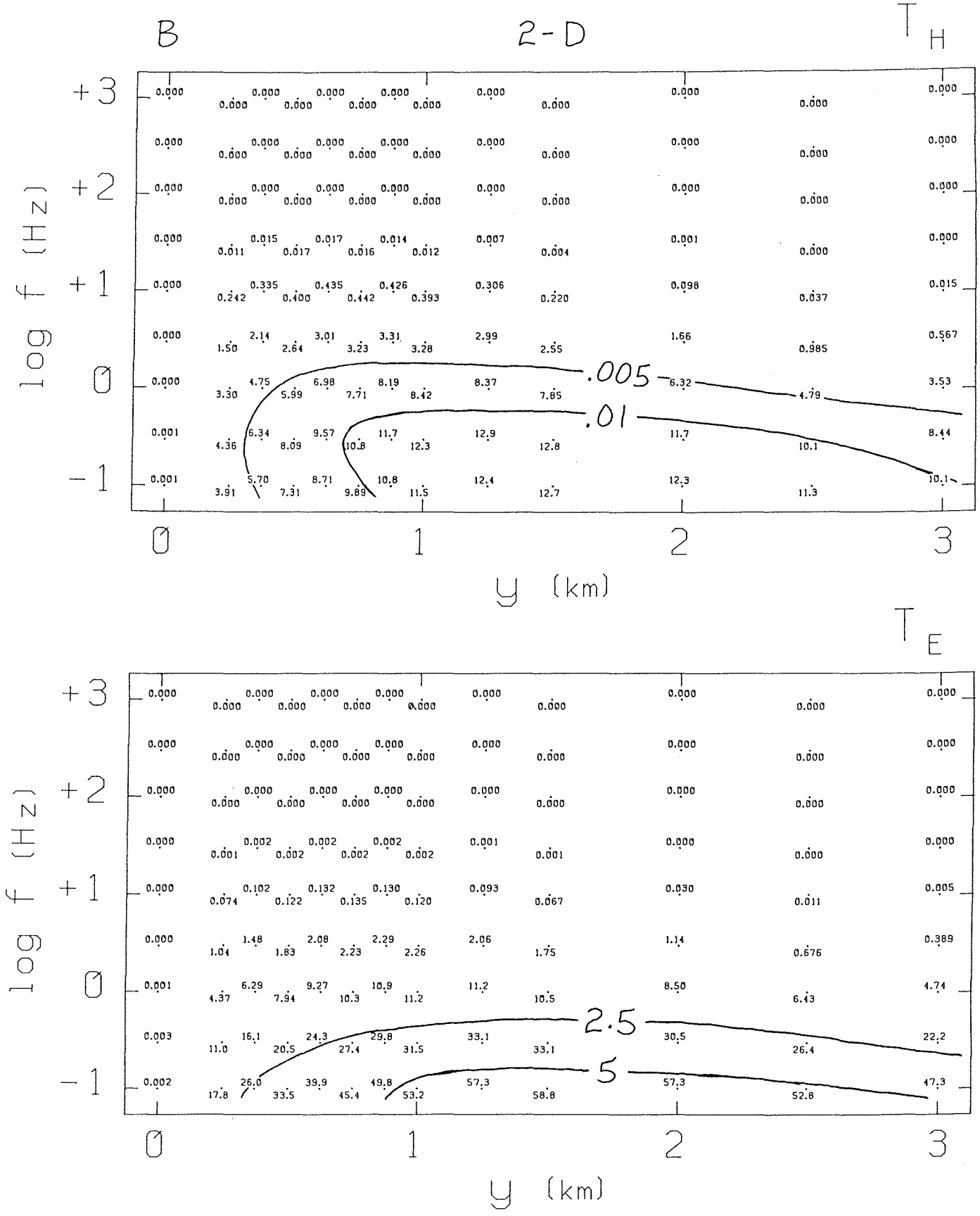

Figure 6. Thick resistive (20 ohm-m) 2-D body buried at a depth of 1 km. a) TE mode. b) TM mode. c). TH, TE.

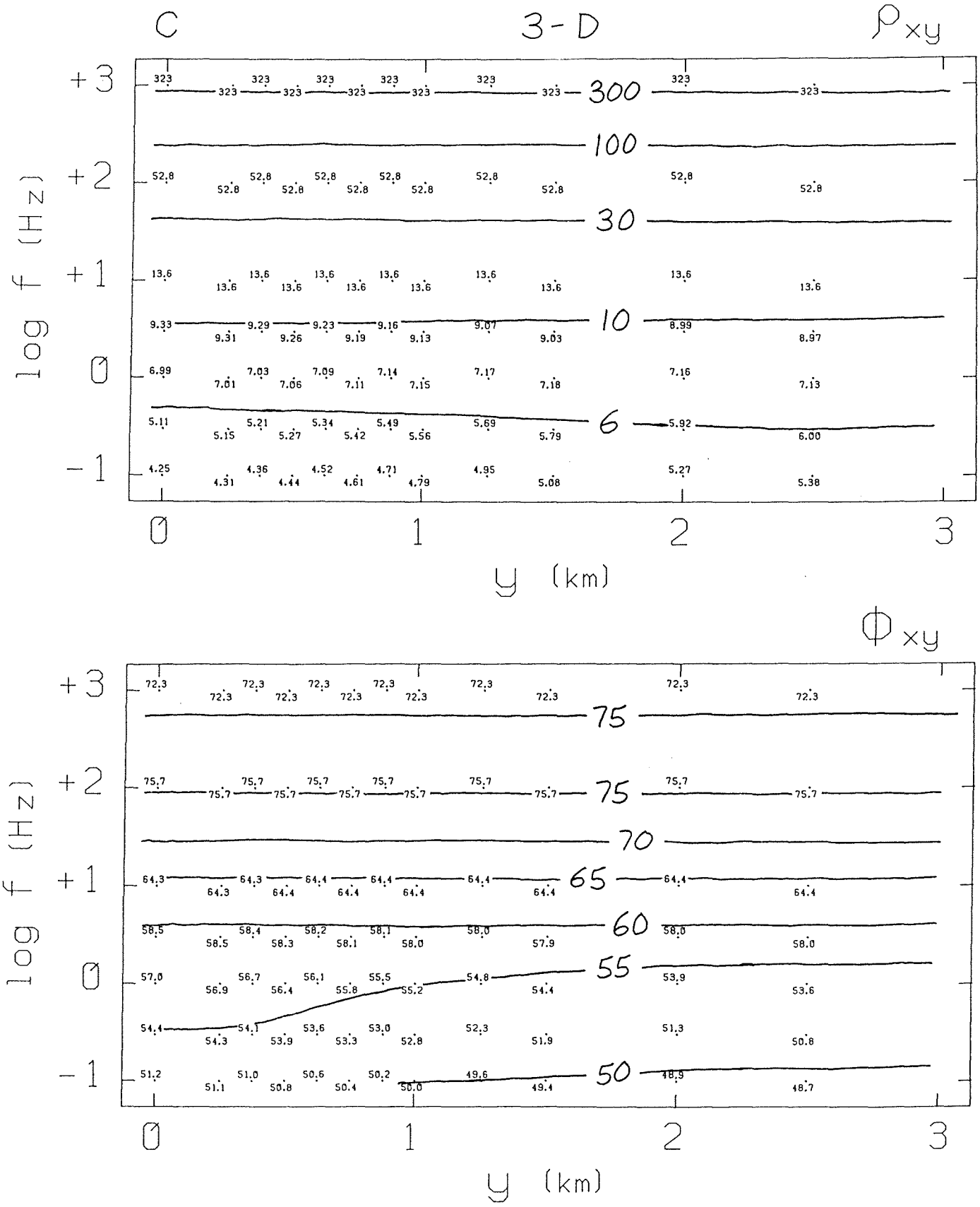

Figure 7. Thin conductive (0.5 ohm-m) 3-D body buried at a depth of 1 km. a) TE mode. b) TM mode. c). TH, TE.

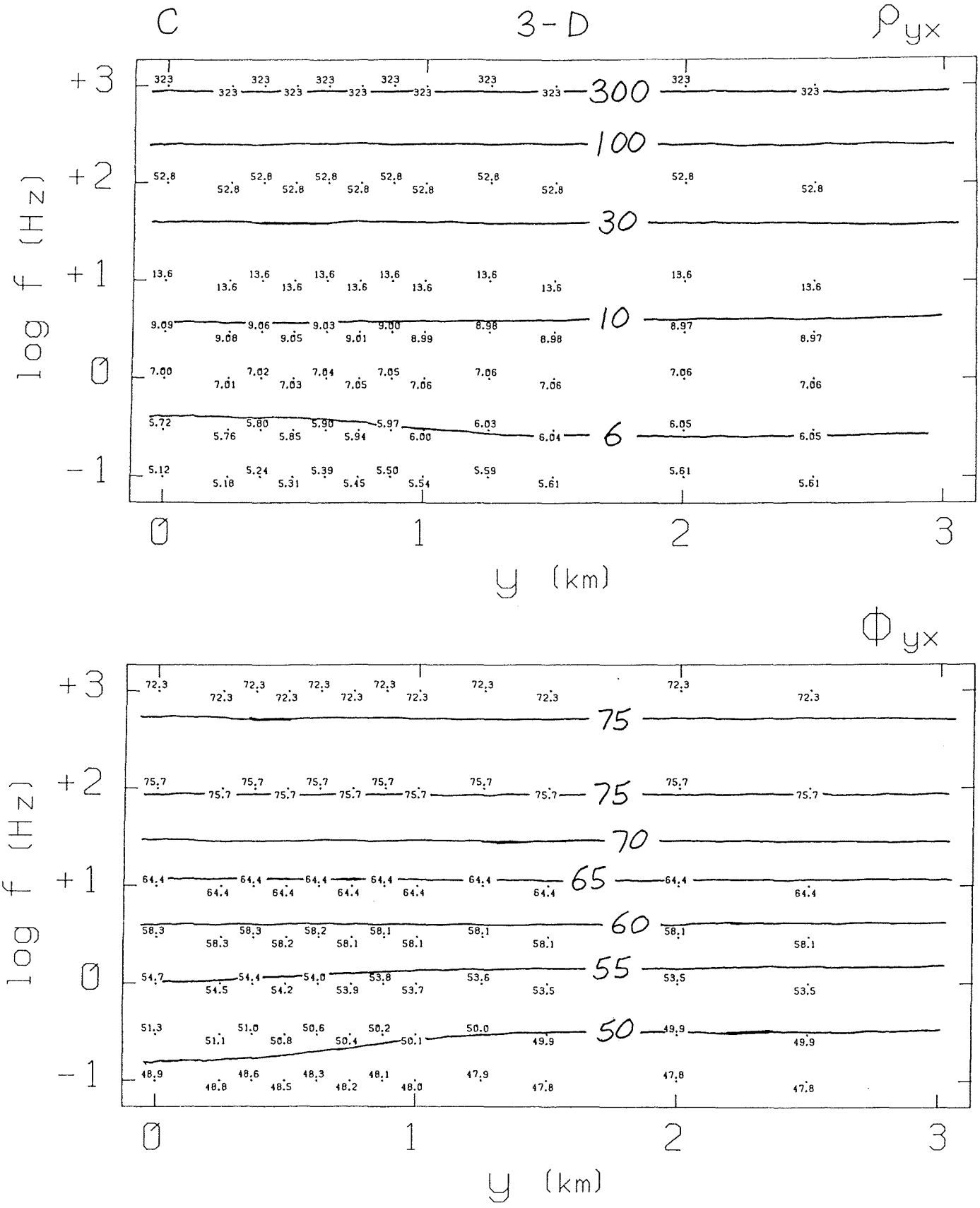

Figure 7. Thin conductive (0.5 ohm-m) 3-D body buried at a depth of 1 km. a) TE mode. b) TM mode. c). TH, TE.

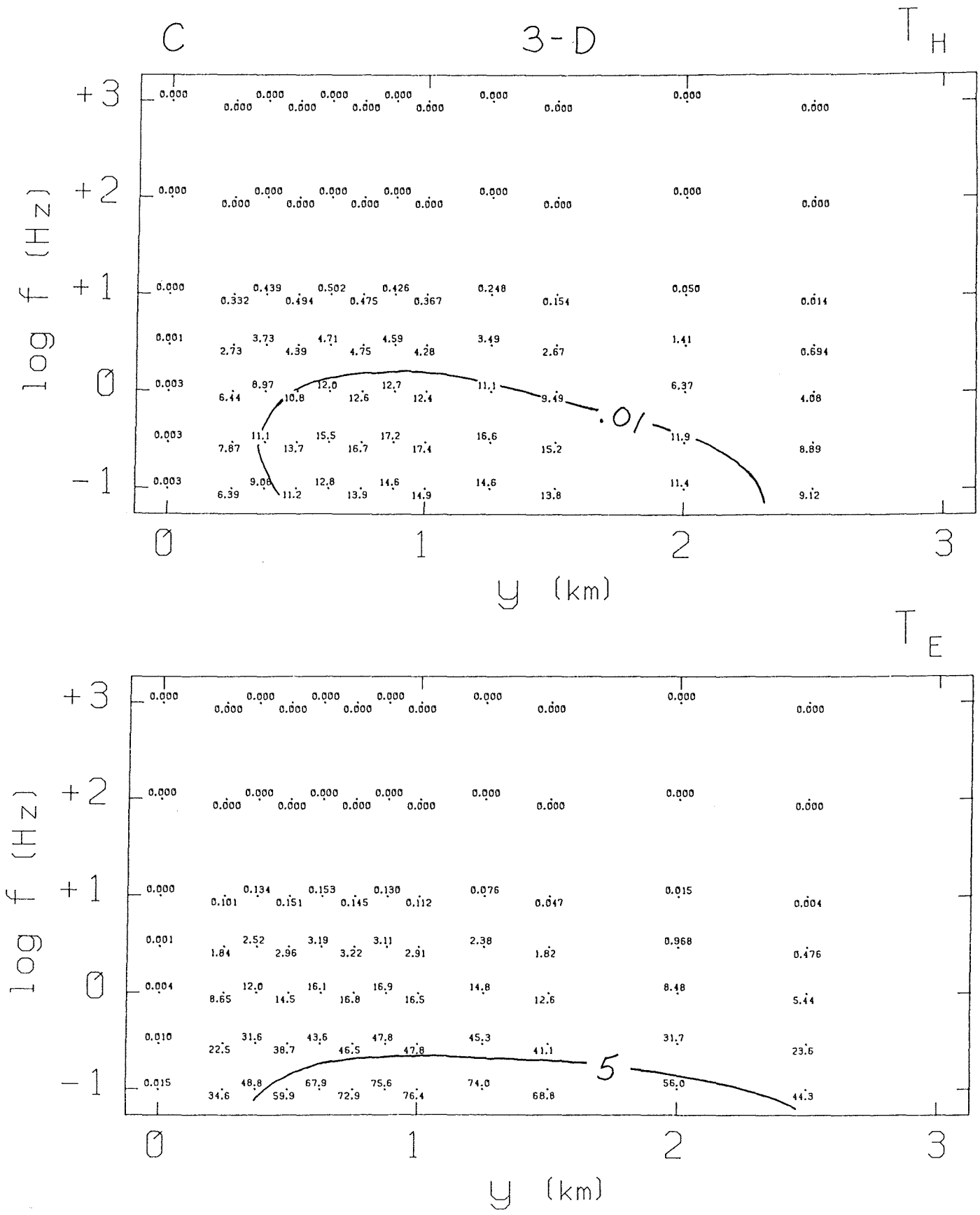

Figure 7. Thin conductive (0.5 ohm-m) 3-D body buried at a depth of 1 km. a) TE mode. b) TM mode. c). TH, TE.

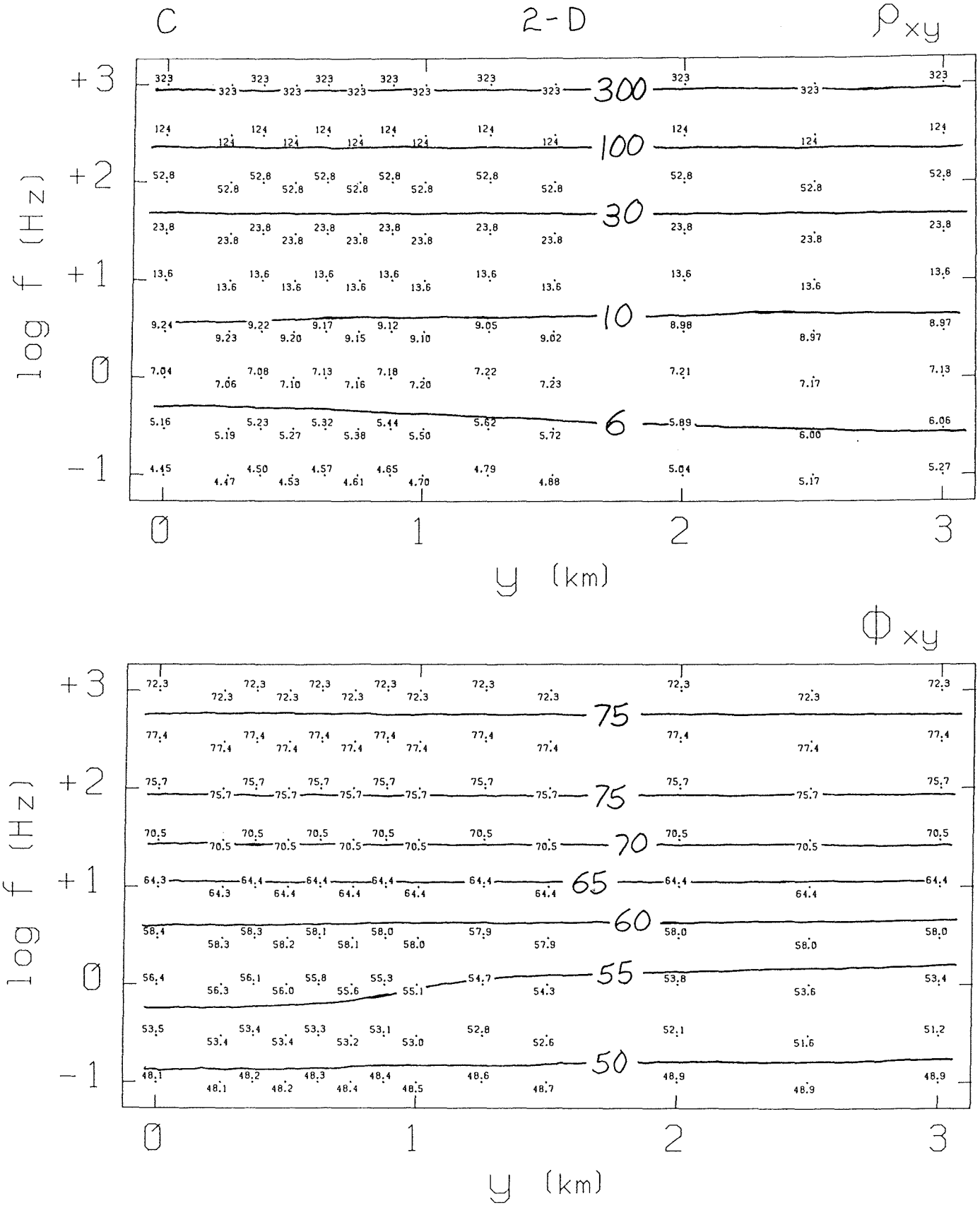

Figure 8. Thin conductive (0.5 ohm-m) 2-D body buried at a depth of 1 km. a) TE mode. b) TM mode. c). TH, TE.

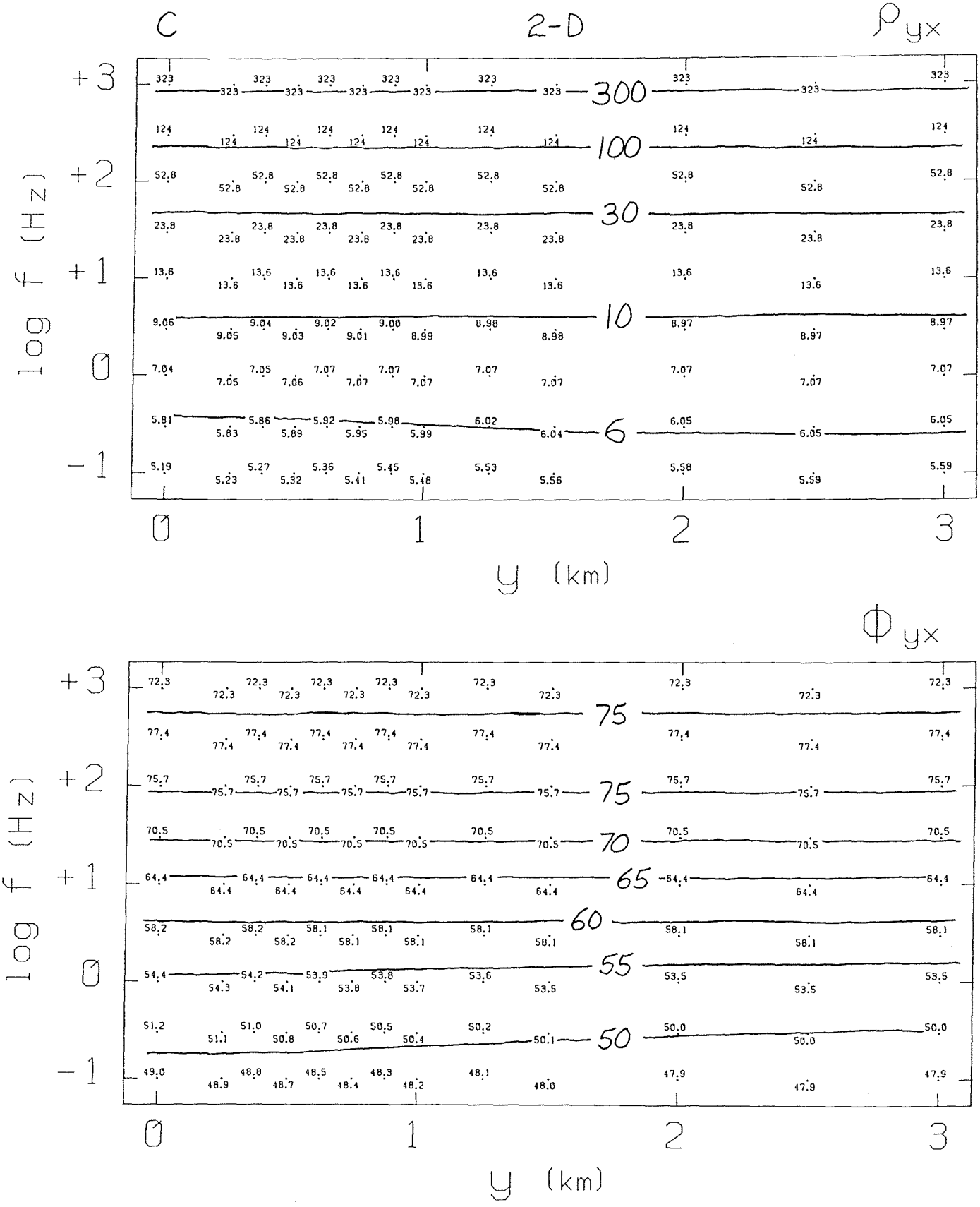

Figure 8. Thin conductive (0.5 ohm-m) 2-D body buried at a depth of 1 km. a) TE mode. b) TM mode. c). TH, TE.

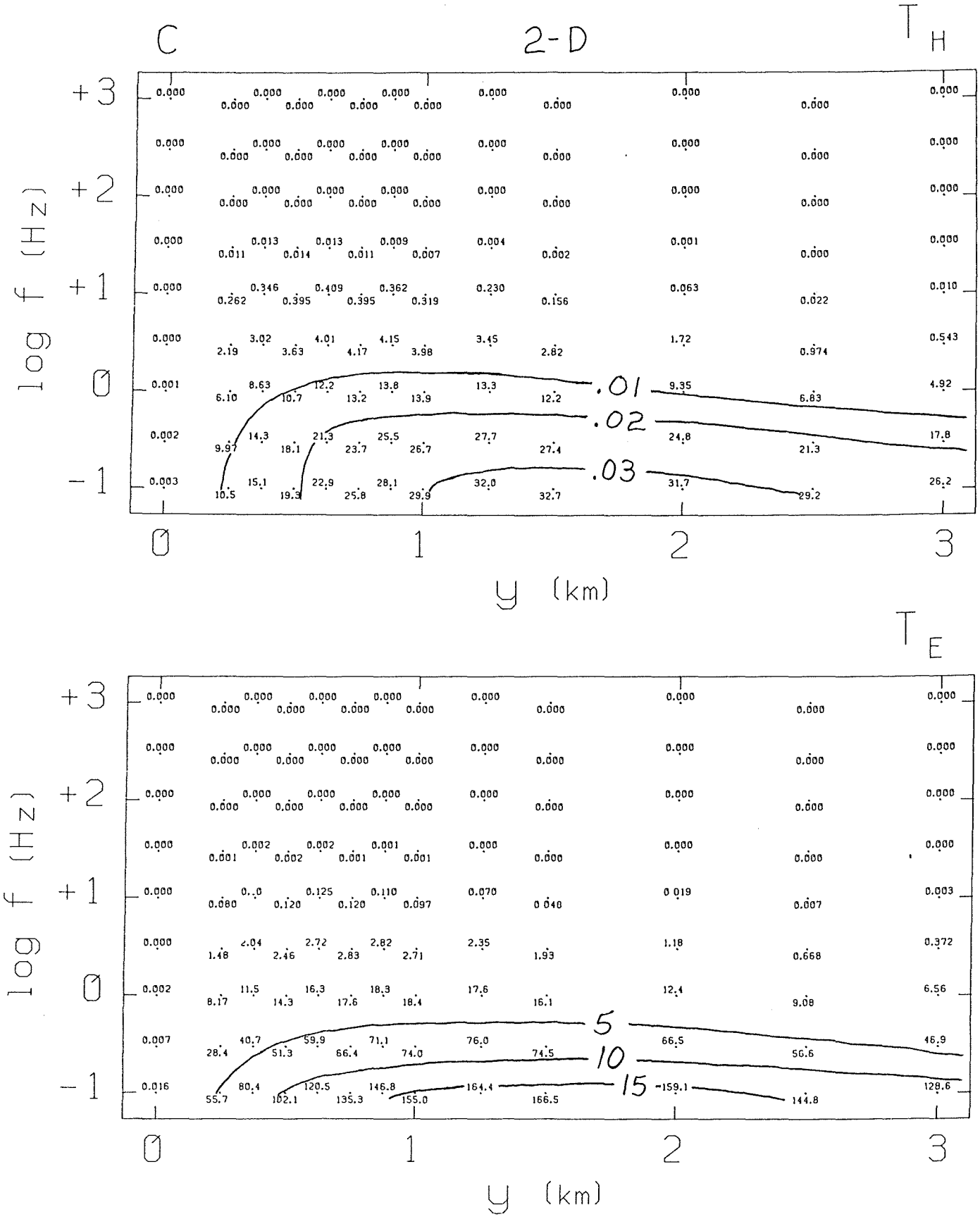

Figure 8. Thin conductive (0.5 ohm-m) 2-D body buried at a depth of 1 km. a) TE mode. b) TM mode. c). TH, TE.

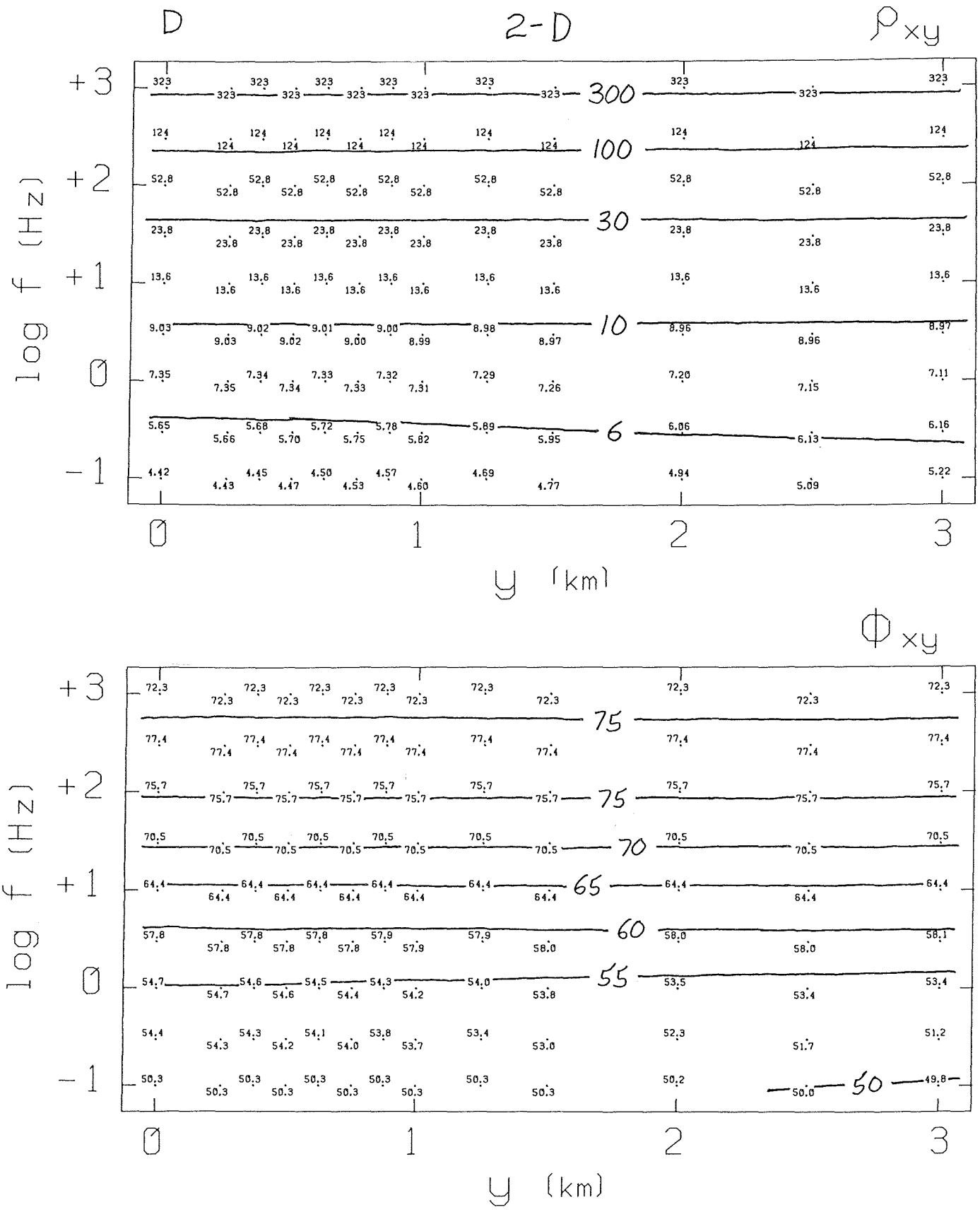

Figure 9. Thick conductive (1 ohm-m) 2-D body buried at a depth of 1.5 km. a) TE mode. b) TM mode. c). TH, TE.

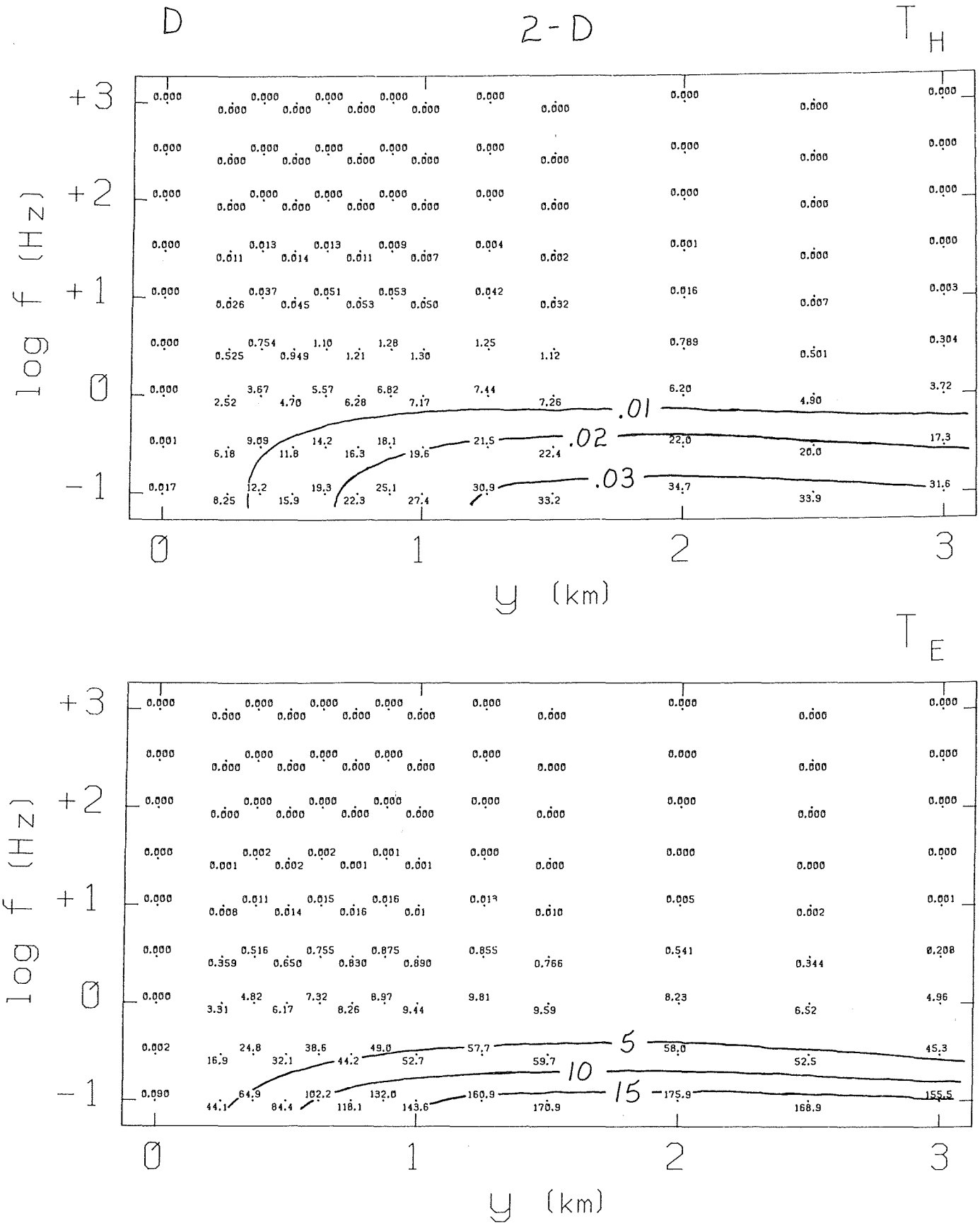

Figure 9. Thick conductive (1 ohm-m) 2-D body buried at a depth of 1.5 km. a) TE mode. b) TM mode. c). TH, TE.

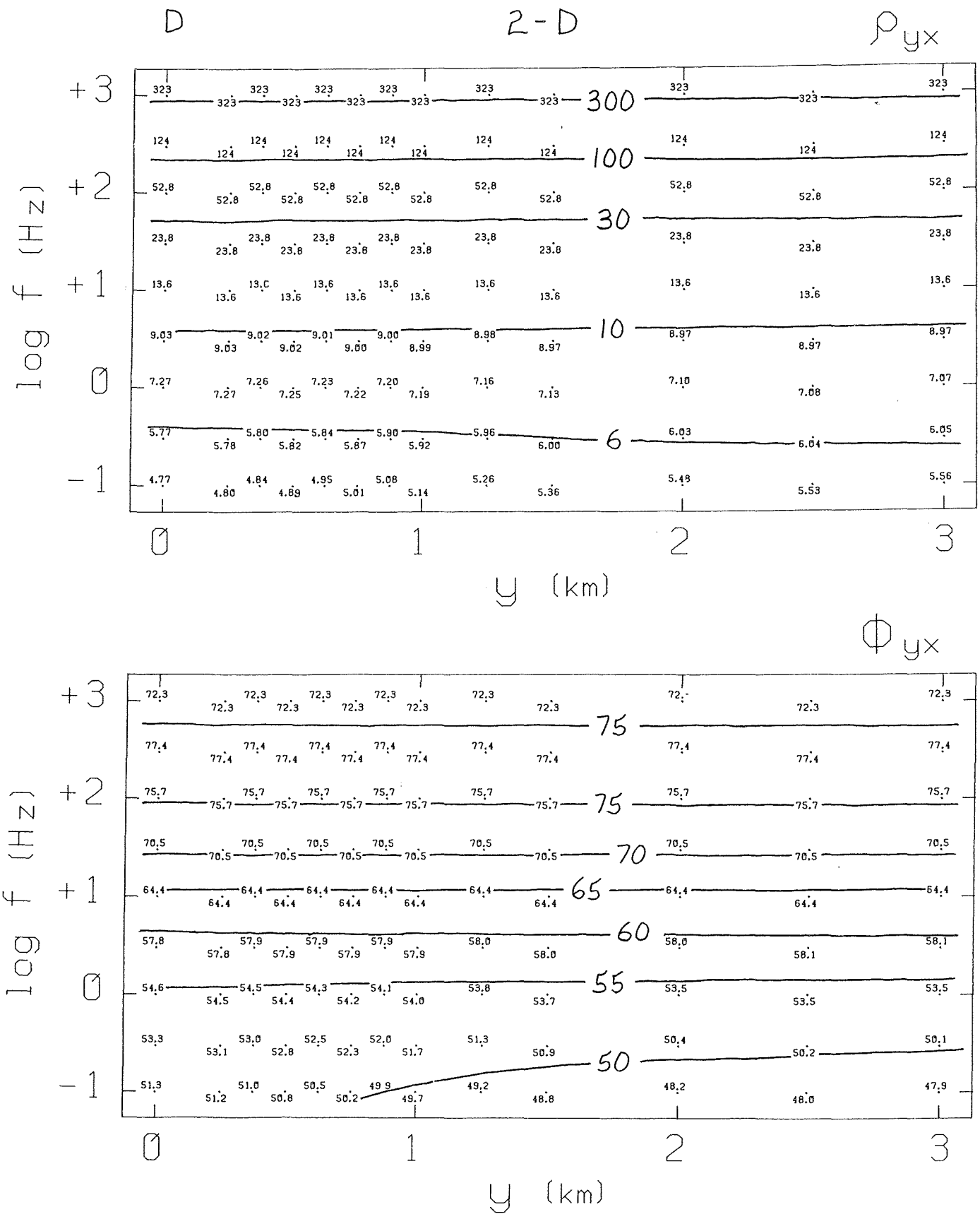

Figure 9. Thick conductive (1 ohm-m) 2-D body buried at a depth of 1.5 km. a) TE mode. b) TM mode. c). TH, TE.